Lifetime measurement of high-wave-number biexcitons in CuCl

K. Kurihara,* E. Tokunaga, M. Baba, and M. Matsuoka,†
The Institute for Solid State Physics, The University of Tokyo, 7-22-1 Roppongi, Minato-ku, Tokyo 106, Japan
(Received 4 November 1994; revised manuscript received 9 May 1995)

We have measured the lifetimes of emissions from biexcitons in CuCl at 2 K whose wave number ranges from $2k_0$ ($\sim 0.89 \times 10^6$ cm^{-1}) to about 6.2×10^6 cm^{-1}. The biexcitons are created via nondegenerate two-photon absorption under a weak excitation condition. M_T emissions show exponential decays that become faster with the wave number, while M_L emissions show slow rise and wave-number-independent decays. These results are analyzed in terms of radiative relaxation, acoustic phonon scattering, and elastic scattering of the biexcitons. The measured lifetimes for the M_T and M_L emissions are assigned to a dephasing time and a population lifetime of the biexcitons, respectively.

I. INTRODUCTION

Biexcitons are elementary excitations described as the bound states of two excitons. Many time-resolved experiments[1–7] have been performed to study the lifetime of biexcitons in CuCl. A recent development of a high-repetition-rate picosecond laser[6] based on cw-mode-locked lasers, whose energy per pulse is 10^{-5} times as weak as previously used laser systems based on Q-switched lasers, has enabled us to make more exact measurements of the lifetime because complicated phenomena accompanying high-density excitations do not occur.

Akiyama *et al.*[4,5] investigated the temporal behavior of biexcitons in CuCl under a weak excitation condition at temperatures between 4.2 and 65 K. In their experiment, annihilation of biexcitons in CuCl gives rise to M_T and M_L emissions, which leave transverse and longitudinal excitons behind in the crystal, respectively. They measured the M_T emission of biexcitons at the wave number $2k_0$ generated by degenerate two-photon resonant absorption, where k_0 is the wave number of the incident photons in the crystal. They found that the relaxation of the biexcitons is ascribed to radiative decay and single-acoustic-phonon scattering. In particular, the radiative lifetime was approximately 50 ps. This value was much shorter than those that had been reported previously.[1–3] In the previous measurements using Q-switched lasers, the decay of the M_T and M_L emissions did not show the biexcitons' own lifetime because the biexcitons were repeatedly produced by collisions among excitons.

In this paper, we report the lifetime measurement of biexcitons in CuCl with higher wave numbers than $2k_0$, ranging from $2k_0$($\sim 0.89 \times 10^6$ cm^{-1}) to about 6.2×10^6 cm^{-1}. We constructed a two-colored laser system, and measured the temporal response of the M_T and M_L emissions of the biexcitons at 2 K generated by nondegenerate two-photon resonant absorption. As a result, we observed differences in the temporal behavior of the M_T and M_L emissions although both of the emissions originate from the same initial biexciton state. Analysis of the results revealed the fundamental relaxation process of biexcitons, which was otherwise difficult to obtain.

II. EXPERIMENTS

Platelets of CuCl single crystal with a thickness of about 10 μm were immersed in superfluid He at 2 K in a strain-free condition. The light source is a uv-picosecond laser system based on sum frequency generation. It delivers synchronous two-colored pulses at a high repetition rate of 82 MHz. Each of the outputs has a spectral width of 0.05 nm, a pulse width of 8 ps, tunability from 375 nm to 395 nm, and an average power of 2 mW. A sample is illuminated by collinear two-colored pulses with a f = 200-mm lens. A polarized beam splitter (PBS) is used to superpose spatially two beams. By putting a $\lambda/4$ plate after PBS, two pulsed beams are made right- and left-handed circularly polarized to satisfy the polarization selection rule of biexcitons in CuCl. They are made spatially and temporally coincident on the sample. The emissions are observed in the backward direction, more exactly, 30° from the backward direction outside of the crystal, about 10° inside of it. Time-integrated spectra are measured with a photomultiplier at an output of a 50-cm monochromator. Time-resolved measurements are carried out with a synchroscan streak camera placed at another port of the monochromator. This system has a time resolution of approximately 20 ps and a spectral resolution of 0.12 nm.

CuCl is a direct gap semiconductor of the zinc-blende structure. It is optically isotropic. The lowest excited state, called the Z_3 exciton state, is split into two degenerate transverse states and one longitudinal state. As a result of strong coupling with photons, the transverse exciton states form an exciton polariton[9] (EP) composed of upper and lower branches. The schematic dispersion curves shown in Fig. 1 explain the excitation and radiative processes of high-wave-number biexcitons. These processes are two-photon transitions that satisfy the energy and momentum conservation laws in the crystal under the restriction of the polarization selection rule. This selection rule is given by the transition probabilities proportional to $|\boldsymbol{e}_1 \cdot \boldsymbol{e}_2|^2$ (Ref. 10) for two photons of polarizations $\boldsymbol{e}_1$ and $\boldsymbol{e}_2$. In the excitation process, the high-wave-number biexcitons can be excited via interme-

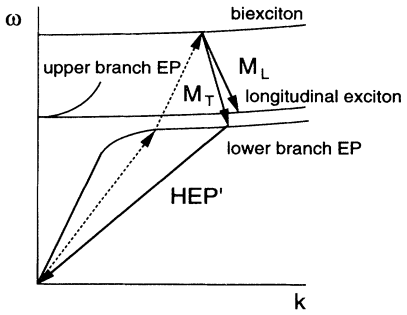

FIG. 1. Schematic of excitation and radiative relaxation processes for high-wave-number excitation of biexcitons. The dashed arrows represent the nondegenerate two-photon excitation. The M_T and M_L arrows are radiative emissions of biexcitons. The HEP′ and M_T arrows are paired emissions.

diate lower branch EP, the wave-number of which can be varied largely by adjusting one of the laser frequencies near the excitonic resonant region, since the dispersion curve is quite horizontal. The two beams are collinear in this experiment, so that the wave number of biexcitons is given as a linear combination of $k_1 + k_2$, where k_1 and k_2 are the wave numbers of two beams in the crystal. In the radiative decay process, the M_T emission leaves the transverse exciton, which is observed as high-energy-peak-dash (HEP′) emission,[11] and the M_L emission leaves the longitudinal exciton, which cannot be observed as radiated emission.

III. RESULTS

Figure 2 shows time-integrated spectra of the high-wave-number biexcitons. The M_T and M_L lines shift to lower energy with the increasing wave number of biexcitons from (a) to (i). At high wave numbers, (e)–(i), the M_T lines overlap with those of the lower energy laser. We could not observe the M_T or M_L emissions of biexcitons beyond 6.2×10^6 cm^{-1} when one of the beams has a higher energy than that of the longitudinal excitons. This could be explained in terms of the onset of the upper branch excitation. When one of the lasers is adjusted to around transverse-exciton energy [3.2022 eV (Ref. 8)], some emissions marked with Ex, Ex-1LO, Ex-2LO, and so on appear. Ex emission is due to excitons accumulated in the bottleneck region situated just below the transverse-exciton energy. Ex-1LO and Ex-2LO emissions are due to one- and two-longitudinal optical phonon relaxation of excitons, respectively. The other emissions seem to be due to bound excitons.

Figure 3 shows the typical results of the time-resolved measurement of the M_T and M_L lines. The M_T intensities have a sharp rise and an exponential decay, while the M_L intensities have a delay in the rising portion and a deviation from the exponential curve at the beginning of the decay. The decay of the M_T lines becomes fast with the increasing wave number of biexcitons. On the other hand the decay of the M_L lines shows no substantial wave-number dependence. In this way the dynam-

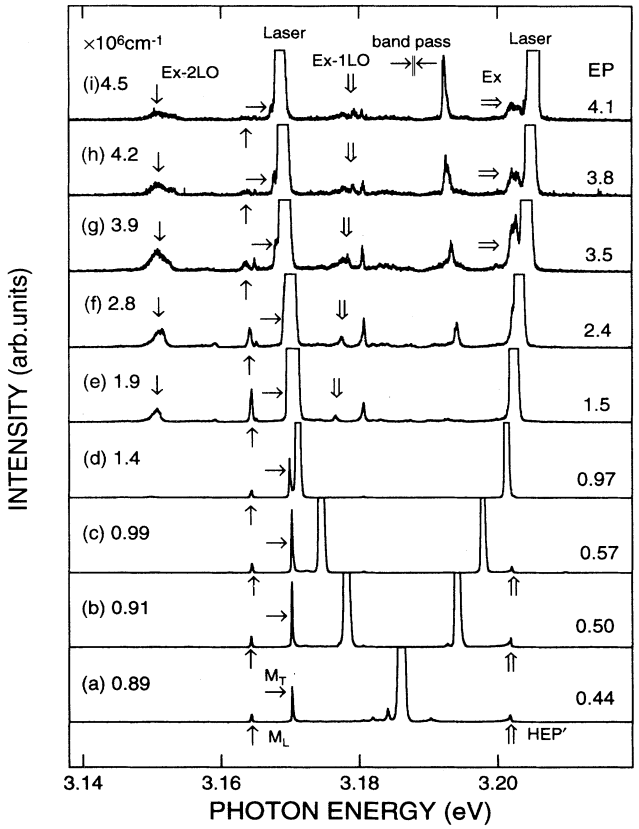

FIG. 2. Time-integrated backward-emission spectra of biexcitons in CuCl with various wave numbers of biexcitons. The wave numbers of biexcitons are indicated on the left and those of EPs excited by higher energy laser on the right.

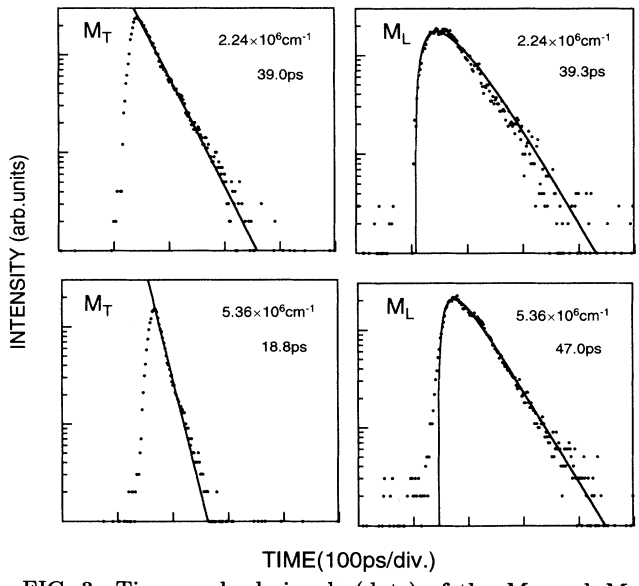

FIG. 3. Time-resolved signals (dots) of the M_T and M_L emissions at two wave numbers of biexcitons in the backward-scattering geometry measured with a synchroscan streak camera. The solid lines and curves are theoretical fits by Eqs. (3) and (5), respectively. Relaxation times of the M_T emissions $\Gamma_{\rm tot}^{-1}$ and the M_L emissions $(\Gamma_{\rm tot} - \Gamma_{\rm el})^{-1}$ are shown in the figures.

ics of the M_T and M_L lines are different, although both emissions originate from the same initial biexciton state.

IV. DISCUSSION

The reason for this difference between the time dependences of the M_T and M_L emissions can be explained by considering the difference in the directional dependence of the two emissions. Analysis[12] of the energy and momentum conservation laws and the polarization selection rule gives the directional dependence of the M_T and M_L emissions. As shown in Fig. 4, the M_T emission is strongest in the direction opposite to the wave vector of biexciton. On the other hand, the M_L emission is forbidden in the direction parallel to it, but is strongest in the perpendicular direction. In our backward observation direction of the initially excited wave vector of the biexcitons, the M_L emission should not be observed. But, in fact, M_L emission is observed. Hence, we must consider the relaxation of the wave vector of the biexcitons due to elastic collisions. The relaxed biexcitons, whose wave vectors have components perpendicular to the initial wave vector, can radiate M_L emissions in the observing direction. Thus, we assume that the biexcitons have a radiative-decay rate $\Gamma_{\rm rad}$, an acoustic phonon scattering rate $\Gamma_{\rm ph}$, and an elastic scattering rate $\Gamma_{\rm el}$. We treat the dynamics of the M_T and M_L emissions by rate equations for N_T, a population of biexcitons having the initially excited wave vector, and N_L, that of elastically scattered biexcitons that lost the initial wave vector. The rate equations are

$$\frac{dN_T}{dt} = -(\Gamma_{\rm rad} + \Gamma_{\rm ph} + \Gamma_{\rm el})N_T, \quad (1)$$

and

$$\frac{dN_L}{dt} = -(\Gamma_{\rm rad} + \Gamma_{\rm ph})N_L + \Gamma_{\rm el}N_T. \quad (2)$$

The solutions to these equations are given by

$$N_T(t) = N_0\exp\{-(\Gamma_{\rm rad} + \Gamma_{\rm ph} + \Gamma_{\rm el})t\} \quad (3)$$

and

$$N_L(t) = N_0\{1 - \exp(-\Gamma_{\rm el}t)\}\exp\{-(\Gamma_{\rm rad} + \Gamma_{\rm ph})t\}. \quad (4)$$

Here, N_0 is an initial population of biexcitons. In Eqs. (1) and (2), we neglect elastic scatterings of N_L back into N_T, which are expressed by a term such as $\alpha\Gamma_{\rm el}N_L$, where α is an appropriate constant. This neglect is allowed because α is much smaller than unity when scatterings in three-dimensional k space are considered. More discussion will be made later after $\Gamma_{\rm el}$ is fitted with data.

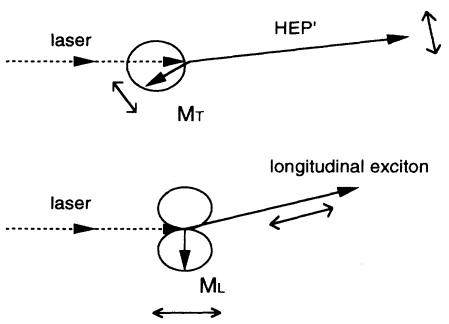

FIG. 4. Schematic of the directional dependence of the M_T and M_L emissions. The directions of polarization are shown by $\leftrightarrow$.

The decay of the M_T emissions is fitted with exponential functions as indicated by the solid lines in Fig. 3. The decay rates thus obtained are assigned to the total relaxation rate $\Gamma_{\rm tot} = \Gamma_{\rm rad} + \Gamma_{\rm ph} + \Gamma_{\rm el}$. In this way, we have obtained $\Gamma_{\rm tot}$ at various wave numbers of biexcitons. After this, the rise and fall parts of the M_L emissions are fitted with the following function:

$$N_L(t) = N_0\{1 - \exp(-\Gamma_{\rm el}t)\}\exp\{-(\Gamma_{\rm tot} - \Gamma_{\rm el})t\}, \quad (5)$$

as indicated by the solid curves in Fig. 3. From this fitting we obtain $\Gamma_{\rm el}$. In these fittings the measured decay curves are not deconvoluted with respect to the laser pulse because the latter have a sharp cut off in the tail compared with the observed exponential decay times. We show the results of $\Gamma_{\rm tot}$ and $\Gamma_{\rm tot} - \Gamma_{\rm el}(= \Gamma_{\rm rad} + \Gamma_{\rm ph})$ in Fig. 5 by filled circles and squares, and open circles and squares, respectively. The circles and squares correspond to the data for two different samples.

The wave-number dependence of $\Gamma_{\rm rad}$, $\Gamma_{\rm ph}$, and $\Gamma_{\rm el}$ are obtained from the literature as in the following.

(i) $\Gamma_{\rm rad}$ is assumed to depend only on the oscillator strength, not on the density of the final states. If the wave function describing the relative motion of two excitons in a biexciton is deuteron type, we obtain as in Ref. 13

$$\Gamma_{\rm rad}(k) = \frac{\Gamma_{\rm rad}(0)}{[1 + (a_{\rm mol}k/2)^2]^2}. \quad (6)$$

Here, k is a wave number of biexcitons, and $a_{\rm mol} = \hbar(m_{\rm mol}G_{\rm mol}/2)^{-1/2}$ is the Bohr radius of the biexcitons, 0.95 nm, where $m_{\rm mol}$ is the translational mass of the biexcitons, $5.29m_e$ (Ref. 8) (m_e is the mass of electron), and $G_{\rm mol}$ is the binding energy of biexcitons, 190 meV.[14] For

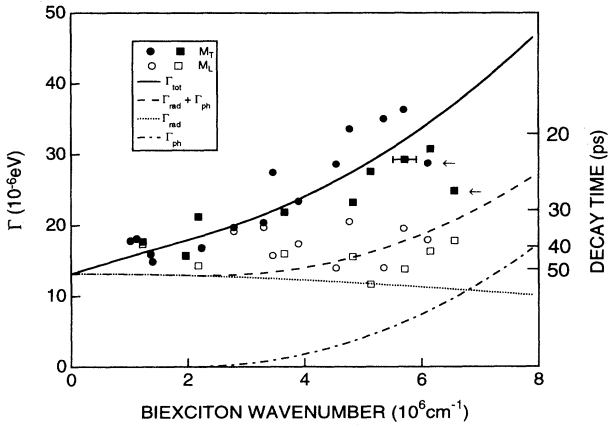

FIG. 5. Plots of the inverse decay-times of the M_T (filled circles and squares) and M_L (open circles and squares) emissions as a function of biexciton wave number. The circles and squares correspond to the data for two samples. The curves are theoretical calculations. Two data points at the highest wave number (indicated by arrows) are regarded as exceptional because of the onset of the upper branch excitation. The error bar is calculated from laser linewidth and the polariton dipersion curve.

$\Gamma_{\rm rad}(0)$, we use the value of $1/(50\ {\rm ps})$.[5] $\Gamma_{\rm rad}(k)$ is plotted in Fig. 5 by the dotted curve.

(ii) $\Gamma_{\rm ph}$ is estimated from the deformation potential interaction, which is the intraband scattering of a biexciton with a spontaneous emission of an acoustic phonon. By referring to Ref. 15, one can derive $\Gamma_{\rm ph}(k)$ as follows:

$$\Gamma_{\rm ph}(k)=\begin{cases}\dfrac{2\pi}{\hbar}\displaystyle\sum_{k'}\dfrac{\hbar E_d^{\rm mol\,2}}{2\rho u V}\delta[\varepsilon(k')-\varepsilon(k)+\hbar u q] \\ \qquad=\dfrac{2m_{\rm mol}E_{\rm d}^{\rm mol\,2}}{3\pi\hbar^2\rho u}\dfrac{(k-k_{\rm c})^3}{k}, \quad (k_{\rm c}<k) \\ 0, \quad (0\le k\le k_{\rm c}),\end{cases} \tag{7}$$

where $\varepsilon(k)$ is the kinetic energy of the biexcitons, $(\hbar k)^2/2m_{\rm mol}$, u is the acoustic velocity, 3.8×10^5 cm/s,[16] q is a wave number of the acoustic phonon, V is the volume, ρ is the density, 4.16 g/cm^3,[17] $E_d^{\rm mol}$ is a deformation potential constant, 0.72 eV,[5] and $k_{\rm c}=m_{\rm mol}u/\hbar=1.65\times10^6$ cm^{-1}.[18] $\Gamma_{\rm ph}(k)$ is plotted in Fig. 5 by the dash-dotted curve. $\Gamma_{\rm rad}(k)+\Gamma_{\rm ph}(k)$ is also plotted in Fig. 5 by the dashed curve, which explains the decay rates of the M_L emission fairly well.

(iii) $\Gamma_{\rm el}$ is calculated from the classical collision theory, and is given by

$$\Gamma_{\rm el}(k)=N_{\rm el}\sigma v_g^{\rm mol}=\frac{N_{\rm el}\sigma\hbar}{M}k, \tag{8}$$

where $N_{\rm el}$ is the density of the elastic scattering centers, σ is the scattering cross section, and $v_g^{\rm mol}=\hbar^{-1}d\varepsilon(k)/dk=\hbar k/m_{\rm mol}$ is the group velocity of the biexcitons. The elastic scattering centers are considered to be mostly impurities and defects.

Now we determine $\Gamma_{\rm el}(k)$ by fitting $\Gamma_{\rm tot}(=\Gamma_{\rm rad}+\Gamma_{\rm ph}+\Gamma_{\rm el})$ to the data points of M_T emissions in Fig. 5. We estimate the inverse of the mean free path, $N_{\rm el}\sigma$, in $\Gamma_{\rm el}$, and find $N_{\rm el}\sigma=(2.1\pm0.2)\times10^4$, and $(1.4\pm0.2)\times10^4$ cm^{-1} for the two samples. In Fig. 5, we use the averaged value $N_{\rm el}\sigma=1.7\times10^4$ cm^{-1}. Two data points at the highest wave number in Fig. 5 (indicated by arrows) are regarded as exceptional because of the onset of the upper branch excitation. Let us consider a simple case where the elastic scattering centers are isolated impurities. If we estimate the cross section by assuming $\sigma=\pi(a+a_{\rm mol})^2$, where a is the lattice constant, 5.4×10^{-8} cm,[19] $N_{\rm el}$ is obtained to be 2.4×10^{17} cm^{-3}. Using the number of atoms per volume in pure CuCl, $N_p=2\rho N_A/M=5.06\times10^{22}$ cm^{-3}, the impurity concentration of $N_{\rm el}/N_p$ is obtained to be 4.7×10^{-6}. Here, N_A is the Avogadro constant and M is the molecular weight of CuCl, 99.0. This ratio is good enough to justify the above decay analysis.

Here, we discuss the validity of Eqs. (1) and (2) in comparison with the results in Fig. 5. When the back flow terms $\alpha\Gamma_{\rm el}N_L$ are included in Eqs. (1) and (2), we find that both N_T and N_L decay with the same rate, $\Gamma_{\rm rad}+\Gamma_{\rm ph}$, when $\Gamma_{\rm el}\gg\Gamma_{\rm rad}+\Gamma_{\rm ph}$ and $t\gg1/\Gamma_{\rm el}$ since directions of biexciton wave vectors then completely randomize. Under these conditions, we are not allowed to neglect the $\alpha\Gamma_{\rm el}N_L$ terms. However, the condition $\Gamma_{\rm el}(k)\le1/(50\ {\rm ps})\simeq(\Gamma_{\rm rad}+\Gamma_{\rm ph})$ of Fig. 5 is not such an extreme case. Thus, Eqs. (1) and (2) hold approximately well within the ranges of the measured time and $\Gamma_{\rm el}(k)$.

We can check thus obtained decay rates by comparing the intensity ratio of M_T to M_L emissions with relaxation constants. Time integration of Eqs. (3) and (4) should give populations of biexcitons contributing M_T and M_L emissions. Taking account of the degree of freedom of polarization for transverse and longitudinal excitons (2:1), we obtain the following relation:

$$I_T:I_L=2(\Gamma_{\rm rad}+\Gamma_{\rm ph}):\Gamma_{\rm el}, \tag{9}$$

where I_T and I_L are time-integrated intensities of the M_T and M_L emissions, respectively. This relation roughly explains the intensity ratios of M_T and M_L emissions in Fig. 2.

We have introduced $\Gamma_{\rm el}$ as the elastic scattering rate, which keeps the population of the biexcitons N_T+N_L constant. After scattering, the biexcitons have three-dimensionally diffused wave-vector components due to their phase changes. This allows us to discuss the decay of the biexcitons in terms of the phase and population relaxation times. The measured lifetime of the M_T emissions corresponds to a dephasing time because of two reasons. First, the observing direction is within the lobe of the M_T emission expected from the energy and momentum conservation laws and the polarization selection rule. Second, the lifetime of the M_T emission is measured at the earliest part of the decay. The measured lifetime of the M_L emissions is a population lifetime because it is the lifetime of the dephased biexcitons.

Akiyama *et al.*[5] found the appearance of the M_T band at the lower energy side of the M_T line of biexcitons at $2k_0$, the latter being our M_T emission in the present study. The M_T band appears at higher temperatures than 4.2 K. The decay time of the M_T band was constant, 50 ps, from 4.2 to 60 K. They concluded that this is the radiative lifetime of biexcitons. (This extraordinarily short lifetime was explained by the giant oscillator strength effect for the transition from a biexciton to an exciton.[5]) The decay time of the M_T line was nearly equal to that of the M_T band at 4.2 K but decreased with increasing temperature. They explained this shortening of decay time in terms of single-acoustic-phonon interaction and obtained a deformation potential constant of 0.72 eV. Our measurement provides more understanding of the elastic scattering relaxation as a function of the biexciton wave number. This relaxation should contribute to the decay time of the M_T line. It should explain a part of the small difference between the decay times of the M_T line at 4.2 K [30 ps (Ref. 4) or 40 ps (Ref. 5)] and the M_T band [50 ps (Ref. 5)].

Kuwata-Gonokami *et al.*[18] reported the wave-number dependence of biexciton linewidth at 1.6 K by the two-photon polarization spectroscopy up to 12×10^6 cm^{-1}. The wave-number dependence of linewidth is consistent with our data in our measured range.

V. CONCLUSIONS

We have performed the picosecond time-resolved spectroscopy of the emissions from biexcitons in CuCl at high

wave numbers. We find that the decay rate of the M_T emission is larger than that of the M_L emission and increases with wave number of biexcitons. Using the assumed decay rates $\Gamma_{\rm rad}$, $\Gamma_{\rm ph}$, and $\Gamma_{\rm el}$ as a function of the wave number, we explain the wave-number dependence of the M_T and M_L emission lifetimes at 2 K. It is concluded that the M_T emission is from cold biexcitons, whereas the M_L emission is from elastically scattered biexcitons.

As an extension to the present study at high wave-numbers, we are conducting the similar measurements at low wave-numbers around $k = 0$ using counterpropagating beam excitation. The results will be reported elsewhere.

ACKNOWLEDGMENT

The authors would like to thank Professor M. Kuwata-Gonokami for his advice to the present work.

* Present address: Kanagawa Academy of Science and Technology, KSP East Rm. 408, 3-2-1 Sakado, Takatsu-ku, Kawasaki-shi, Kanagawa-ken 213, Japan.

† Present address: Faculty of Science, Kumamoto University, 2-39-1 Kurogami, Kumamoto-shi, Kumamoto-ken 860, Japan.

[1] M. Ojima, T. Kushida, S. Shionoya, Y. Tanaka, and Y. Oka, J. Phys. Soc. Jpn. **45**, 884 (1978).

[2] Y. Masumoto, S. Shionoya, and Y. Tanaka, Solid State Commun. **27**, 1117 (1978).

[3] Y. Segawa, Y. Aoyagi, O. Nakagawa, K. Azuma, and S. Namba, Solid State Commun. **27**, 785 (1978).

[4] H. Akiyama, M. Kuwata, T. Kuga, and M. Matsuoka, Phys. Rev. B **39**, 12 973 (1989).

[5] H. Akiyama, T. Kuga, M. Matsuoka, and M. Kuwata-Gonokami, Phys. Rev. B **42**, 5621 (1990).

[6] T. Kuga, H. Akiyama, M. Kuwata-Gonokami, and M. Matsuoka, in *Optical Properties of Solids*, edited by K.C. Lee, P.M. Hui, and T. Kushida (World Scientific, Singapore, 1991), p. 109.

[7] T. Ikehara and T. Itoh, Solid State Commun. **79**, 755 (1991).

[8] T. Mita, K. Sôtome, and M. Ueta, J. Phys. Soc. Jpn. **48**, 496 (1980); Solid State Commun. **33**, 1135 (1980).

[9] J.J. Hopfield, Phys. Rev. **112**, 1555 (1958).

[10] E. Doni, R. Girlanda, and G. Pastri Parravicini, Solid State Commun. **17**, 189 (1975).

[11] T. Itoh, T. Suzuki, and M. Ueta, J. Phys. Soc. Jpn. **42**, 1069 (1977).

[12] F. Henneberger, K. Henneberger, and J. Voigt, Phys. Status Solidi B **83**, 439 (1977).

[13] A.A. Golovin and E.I. Rashaba, Pis'ma Zh. Eksp. Teor. Fiz. **17**, 690 (1973) [JETP Lett. **17**, 478 (1973)].

[14] A. Goladmann, Phys. Status Solidi B **81**, 9 (1977).

[15] K. Seeger, *Semiconductor Physics* (Springer-Verlag, Berlin, 1989), p. 168.

[16] Y. Masumoto and S. Shionoya, J. Phys. Soc. Jpn. **51**, 181 (1982).

[17] T.H.K. Barron, J.B. Birch, and G.K. White, J. Phys. C **10**, 1617 (1977).

[18] M. Kuwata-Gonokami, R. Shimano, J. Iwamatsu, H. Akiyama, T. Kuga, and M. Matsuoka, Phys. Status Solidi B **159**, 347 (1990).

[19] J.N. Plendel and L.C. Mansur, Appl. Opt. **11**, 1194 (1972).